Phenotypic screening using waveform analysis of calcium dynamics in primary cortical cultures

Richi Sakaguchi [1, *], Saki Nakamura [2], Hiroyuki Iha [3], Masaki Tanaka [1, *]

[1] Department of Lead Discovery Research, New Drug Research Division, Otsuka Pharmaceutical Co., Ltd., Kagasuno, Tokushima, Japan

[2] Department of Research Management, New Drug Research Division, Otsuka Pharmaceutical Co., Ltd., Kagasuno, Tokushima, Japan

[3] Office of Bioinformatics, Department of Drug Discovery Strategy, New Drug Research Division, Otsuka Pharmaceutical Co., Ltd., Kagasuno, Tokushima, Japan

* Corresponding Authors
Email: Sakaguchi.Richi@otsuka.jp (Richi Sakaguchi)
Email: Tanaka.Masaki@otsuka.jp (Masaki Tanaka)

Abstract

At present, *in vitro* phenotypic screening methods are widely used for drug discovery. In the field of epilepsy research, measurements of neuronal activity have been utilized for predicting efficacy of anti-epileptic drugs. Fluorescence measurements of calcium oscillations in neurons are commonly used for measurement of neuronal activities, and some anti-epileptic drugs have been evaluated using this assay technique. However, changes in waveforms were not quantified in previous reports. Here, we have developed a high-throughput screening system containing a new analysis method for quantifying waveforms, and our method has successfully enabled simultaneous measurement of calcium oscillations in a 96-well plate. Features of waveforms were extracted automatically and allowed the characterization of some anti-epileptic drugs using principal component analysis. Moreover, we have shown that trajectories in accordance with the concentrations of compounds in principal component analysis plots were unique to the mechanism of anti-epileptic drugs. We believe that an approach that focuses on the features of calcium oscillations will lead to better understanding of the characteristics of existing anti-epileptic drugs and allow prediction of the mechanism of action of novel drug candidates.

Introduction

The central nervous system (CNS) has critical roles in homeostatic regulation. In recent decades, therefore, many CNS drugs have been developed. Historically, *in vivo* screening was used in the early stage of drug discovery, while *in vitro* functional screening systems have recently been developed and have contributed to increasing throughput. For example,

phenotypic differences in morphological parameters and protein aggregation detected by a high-content imaging system were applied in discovering ALS drug candidates [1]. In addition, neuronal activities including membrane potential and postsynaptic currents were also used to develop compounds that act on ion channels, using a plate reader system and an automated patch clamp system [2].

Epilepsy is a type of neurological disorder. It has been reported that epileptic neuronal activity was induced by lowering magnesium concentrations in neocortical slices [3], because this condition increased the activity of N-methyl-D-aspartate (NMDA) receptors and caused seizure-like activity. As a phenomenon that reflects neuronal activity, calcium oscillations were often used [4]. Synchronized calcium oscillations were observed in cultured cortical neurons [5], [6] and calcium oscillations are driven by bursts of action potentials in neuronal cultures [7]. A previous report showed that calcium oscillations had the potential to be incorporated into phenotypic screening methods for characterizing some compounds including AEDs [8]. However, lack of quantitation complicated the interpretation of the experimental results. As an improvement, we have developed a new high-throughput screening system that uses the signals of calcium oscillations in cultured cortical neurons, which mimic epileptic activity.

In the present study, we achieved simultaneous measurement of calcium oscillations in 96-well plates, using an FDSS/μCell to optimize high-throughput screening. Moreover, we quantified the number and the shape of calcium oscillations as automatically extracted features and classified commonly used AEDs based on their mechanism of actions (MoAs).

Materials and methods

Ethic statement

All experiments involving animals were performed in accordance with "Guidelines for Animal Care and Use in Otsuka Pharmaceutical Co, Ltd."

Compounds

Perampanel and lacosamide were synthesized at Otsuka Pharmaceutical Co., Ltd. Levetiracetam (#L0234) was purchased from Tokyo Chemical Industry Co., Ltd.; brivaracetam (#B677645) from Toronto Research Chemicals; diazepam (#D0899) from SIGMA; clonazepam (#038-17231) from FUJIFILM Wako Pure Chemical Corporation; lamotrigine (#L0349) from LKT Laboratories. All compounds were dissolved in dimethyl sulfoxide (DMSO) (#043-07216, FUJIFILM Wako Pure Chemical Corporation) to make up stock solutions.

Reagents

The composition of Tyrode's buffer was 140 mM NaCl, 4 mM KCl, 1.8 mM $CaCl_2$, 5 mM HEPES, 0.33 mM NaH_2PO_4, 0.1 mM $MgCl_2$ and 5.5 mM glucose. HEPES was purchased from Dōjindo Laboratories; NaCl, KCl, $CaCl_2$, NaH_2PO_4, $MgCl_2$ and glucose from FUJIFILM Wako Pure Chemical Corporation. B-27™ Plus Neuronal Culture System (#A3653401, Gibco) containing penicillin-streptomycin solution (#P4333, Sigma-Aldrich) was used to culture primary cells, and Neurobasal medium (#21103-049, Gibco) containing B27 supplement (#17504044, Gibco), GlutaMAX (#35050061, Gibco) and penicillin-streptomycin solution was used to harvest the cells.

Primary neuronal culture

Rat primary cortical neuronal cultures were established from rat embryos (Crl: CD (SD)) at embryonic day 18. The cortical neurons were dissected using the Papain Dissociation System (Worthington Biochemical Corp). In brief, brain cortex was collected in ice-cold HBSS and dissociated in 0.25% papain/Dnase I in PBS for 30 minutes in the incubator, Neurobasal medium was added to 10 mL and pipetted 10 times. The supernatant was collected, filtrated using a cell strainer (#352350, Falcon), and centrifuged (1,000 rpm, 5 min). The pellet was suspended in Ovomucoid protease inhibitor/HBSS, centrifuged (800 rpm, 5 min) and resuspended in the medium for harvesting.

The dissociated cells were seeded onto 60 wells (all wells except the perimeter wells on 96-well plates (#3842, Corning)) at a density of 75,000 cells/well. Cell cultures were maintained inside a 5% CO_2 incubator at 37˚C and half of the medium was replaced once every 3-4 days. For all experiments, cultures were used at 14 days *in vitro* (DIV 14)**.**

Calcium imaging

A vial of Cal-520 (#21130, AAT-Bioquest) was resuspended to 2 µM in Tyrode's buffer (0.1 mM Mg^{2+}) containing 0.01% Pluronic F-127 (#P3000MP, Invitrogen). The cultures were washed three times in Tyrode's buffer, and incubated in 80 µL of Cal-520 per well for 1 hour at 37°C. Culture plates were set to an assay stage and stabilized for more than 10 minutes before measurement.

For calcium imaging, an FDSS/µCell (Hamamatsu Photonics) kinetic plate reader was used. After incubation, 20 µL of compounds dissolved in Tyrode's buffer were dispensed using the 96 dispenser head of the FDSS/µCell and, 5 minutes after dispensing, calcium signals were measured for 5 minutes using the following settings: exposure time 36.5 ms,

121 excitation wavelength 480 nm, emission wavelength 540 nm, temperature controlled at
122 37°C.
123

124 Data analysis

125 Fluorescence intensity data were extracted using FDSS/μCell software. Data analysis and
126 visualization were processed using the "Wave Finder" in Spotfire (Data Visualization &
127 Analytics Software—TIBCO Spotfire, http://spotfire.tibco.com/) and custom code
128 written in R for PCA. PCA features were selected based on correlation of features and
129 visual inspection of each waveform. Statistical analysis of each feature was performed
130 and visualized with GraphPad Prism 7 (GraphPad Software).
131
132

133 Results

134 Synchronized calcium oscillations were detected 135 simultaneously under 60 conditions.

136 In previous reports, spontaneous intracellular calcium oscillations of cultured neurons in
137 96-well plates have been observed [8], [9]. To reproduce *in vitro* calcium oscillations in
138 our laboratory, we determined the appropriate experimental conditions in our laboratory
139 setting. We cultured rat primary cortical neurons in 96-well plates and observed calcium
140 oscillations using the fluorescent calcium indicator Cal-520 dissolved in Tyrode's buffer
141 at DIV 14 (Fig 1A). To mimic epilepsy-like neuronal activity, low magnesium (0.1 mM)
142 Tyrode's buffer was used in our assays [9]–[11]. We have succeeded in observing
143 synchronized calcium oscillations in 60 wells simultaneously using the FDSS/μCell. In
144 each well, more than 40 peaks were observed over 5 minutes. We therefore decided to

measure calcium oscillations under these conditions for all subsequent pharmacological experiments.

Fig 1. The schema for simultaneous measurement of calcium oscillations in 96-well plates and methods for extracting wave features.

(A) Schematic of our method for measurement of calcium oscillations. Rat primary cortical neurons were harvested and cultured to DIV 14. Cultures were loaded with calcium indicator Cal-520 and measured in 60 wells (all except the perimeter wells on 96-well plates). (B) A representative calcium oscillation and definitions of wave features. Calcium oscillations were visualized and each feature extracted using Wave Finder in Spotfire. Features are defined as follows. Mean Peak Height is the difference between the maximum value of the peak and the height of the point at which the peak starts rising. Mean Peak Height / Peak Width was the ratio of the peak height to the peak width. Peak Width was the time from the point at which the peak starts rising to the time when the signal decreased to 10% of the peak height. Mean Peak Width 50% was the time from the maximum value to the time when the signal decreased to the half of this value. AUC was calculated using the trapezoidal rule. (C) The list of features extracted from calcium oscillations.

Features extracted from calcium oscillations can characterize anti-epileptic drugs.

It was reported that calcium oscillations were affected by compounds, which modulate the activity of ion channels [8], [9]. In particular, the frequency and shape of calcium

169 oscillations varied depending on the compound. We considered a phenotypic cell-based
170 assay for characterizing AEDs using calcium oscillations. To evaluate the shapes of
171 calcium oscillations, we extracted six features of the waves using Wave Finder software
172 (Fig 1B). The features are mean peak height (Mean Peak Height), coefficient of variation
173 (CV) of peak height (CV of Peak Height), the ratio of peak height to peak width (Mean
174 Peak Height / Peak Width), the peak width from the time of the maximum value to the
175 time when the signal drops to half of this value (Mean Peak Width 50%), total area under
176 the curve (AUC), and the number of peaks (Peak Number) in each well. These six features
177 were extracted for all detected peaks. We used positive allosteric modulators (PAM) of
178 GABAergic inhibitory activity, diazepam (10 μM) and clonazepam (10 μM), inhibitors
179 of excitatory inputs via voltage-gated sodium channels, carbamazepine (30 μM),
180 lamotrigine (10 μM) and lacosamide (100 μM), and the widely used AEDs levetiracetam
181 (100 μM), brivaracetam (100 μM) and perampanel (10 μM) to characterize their features
182 (Fig 2A). The concentration of each compound was selected according to the therapeutic
183 range of the concentration in plasma [12]. Each compound was applied to 6 wells in a
184 plate by the FDSS/μCell auto-dispenser, incubated for 5 minutes and the signals of
185 calcium oscillations recorded for 5 minutes. Compared to wells treated with DMSO
186 (0.1%), the waveforms of calcium oscillations in wells to which some compounds were
187 treated varied (Fig 2B). We calculated features from all detected peaks by Wave Finder
188 software and confirmed that features were changed substantially (Fig 2C). For example,
189 mean peak heights significantly decreased in wells treated with perampanel, diazepam,
190 clonazepam or carbamazepine, but increased in wells to which brivaracetam, lamotrigine,
191 and lacosamide were applied. In addition, peak numbers increased on treatment with
192 diazepam, clonazepam, lamotrigine and lacosamide. Conversely, no features were

193 changed on treatment with levetiracetam. The results were consistent with the previous
194 report [8]. We could thus characterize these AEDs by the features of the peaks of their
195 calcium oscillations.
196
197 **Fig 2. The changes of wave features in response to treatment with AEDs.**
198 (A) Summary of the AEDs used in our calcium oscillations assay. (B) Representative
199 recordings of calcium oscillations exposed to DMSO or several AEDs. X-axis represents
200 peak heights in arbitrary units (a.u.), while y-axis represents time in seconds.
201 (C) Bar plots of features extracted from wells to which AEDs were applied. Features were
202 calculated from 6 wells per AED containing DMSO. Data are means ± SEM (n = 6 wells).
203 p*<0.05 vs. DMSO (n = 48-169 peaks per well, one-way ANOVA with Dunnett post-hoc
204 test).
205
206 To characterize these drugs robustly, we next compared the features of calcium
207 oscillations caused by compounds using PCA. PCA is a useful method for evaluating
208 multiple features simultaneously. The PCA plots showed that the clusters of some
209 compounds were clearly segregated (Fig 3A). The relative contributions of the principal
210 components and contribution of the different features to the PC1 and PC2 are depicted in
211 Fig 3B and 3C, respectively. Two components have an eigenvalue more than 1. Together,
212 two components explained 84.8% of the variability. The CV of the Peak Height and Peak
213 Number made a positive contribution and the Mean Peak Height, Mean Peak Height /
214 Peak Width, and AUC contributed negatively to PC1. We therefore suggest that these
215 features were critical for differentiating PAMs of $GABA_A$ receptors. In addition, Mean
216 Peak Width 50% made a strong contribution to PC2 and this feature had a large effect on

segregating inhibitors of excitatory inputs. On the other hand, levetiracetam and brivaracetam were not segregated from DMSO. This is reasonable because their features were not substantially changed, compared with DMSO. Thus, AEDs were characterized by the features of calcium oscillations.

Fig 3. PCA coordinates and contribution plots in response to treatment with AEDs.
(A) PCA of wave features. The individual wells are plotted. Different AEDs are represented by different shapes.
(B) Plot depicting the contribution of features to PC1 and PC2 (arrows).
(C) Bar plot displaying the percentage of variance explained by each component.

The concentration of a compound is critical in determining the features of calcium oscillations.

Next, we examined the concentration dependence of each compound. Levetiracetam and brivaracetam were excluded from this experiment because these compounds had negligible effects on the features of calcium oscillations in previous assays. We applied 6 compounds at 3 concentrations to 3 wells per condition, including DMSO at a single concentration. We extracted features from all detected peaks using the previous methodology (Fig 4). On PCA plots, plots at low concentrations were located near the DMSO plot (Fig 5A). The contribution ratio of principal components and the contribution of the different features to the PC1 and PC2 is depicted in Figures 5B and 5C, respectively. As the concentration increased, plots were separated from the DMSO plot. As we expected, specific compounds move along different trajectories. Moreover, the clusters

241 of diazepam and clonazepam, targeting the GABA receptor, moved in the same directions
242 as concentrations increased. A similar tendency was seen with lamotrigine, lacosamide
243 and carbamazepine because their targets are voltage-gated sodium channels. Additionally,
244 the trajectory of perampanel moved in a similar direction to that of sodium channel
245 blockers. The target of perampanel is the AMPA receptor, which mediates excitatory
246 synaptic transmission. Both sodium channel blockers and AMPA receptor antagonists
247 inhibit neurohyperexcitability. These findings therefore suggest that our method reflected
248 their MoA to some extent. Our method allowed us to characterize AEDs based on their
249 MoAs.
250
251 **Fig 4. The changes of wave features in response to treatment with AEDs at three**
252 **concentrations.**
253 Bar plots of features extracted from wells to which AEDs were treated. Features were
254 calculated and averaged from 3 wells per AED under each condition, also containing
255 DMSO. Data are means ± SEM (n = 3 wells). p*<0.05 vs. DMSO (n = 44-166 peaks per
256 well, one-way ANOVA with Dunnett post-hoc test).
257
258 **Fig 5. Trajectories of PCA plots in accordance with concentrations of AEDs.**
259 (A) PCA of wave features. The centers of wells are depicted under the same conditions.
260 Different AEDs display different shapes. Light colors depict low concentrations, whereas
261 dark colors represent high concentrations. Plots of the same AEDs are connected by lines
262 in order of the concentration used.
263 (B) Plot depicting the contribution of features to PC1 and PC2 (arrows).
264 (C) Bar plots displaying the specific proportion of total variance explained by each PC.

Discussion

It is known that intracellular calcium oscillations partially reflect neuronal activity [7]. In previous reports, calcium oscillations of cortical cultures were used as functional assays for drug screening [8], [9], [11], and changes were observed in calcium oscillations when several AEDs, such as GABA receptor agonists and inhibitors of excitatory inputs, were applied [8]. In this report, we quantify differences between AEDs using waveforms of calcium oscillations and classify their mechanisms based on their effects on excitatory inputs and inhibitory inputs.

Our method used features extracted by automatically quantifying the shape and number of calcium oscillations. The six features we used were sufficient for characterizing some AEDs. In addition, our assay was able to characterize AEDs based on their MoAs because PCA plots of diazepam and clonazepam were located near certain coordinates and moved along similar trajectories in a concentration-dependent manner. Lamotrigine and lacosamide, known to be voltage-gated sodium channel blockers, also showed similar trajectories. In contrast, carbamazepine was segregated from them. The difference is possibly because carbamazepine has effects both on $GABA_A$ receptors as a positive allosteric modulator and on GABA release [13], [14]; while few studies report that lamotrigine and lacosamide have effects on GABA currents with acute treatment. In addition, we could not observe substantial changes in calcium oscillations due to levetiracetam or brivaracetam. In some *in vitro* epileptic models, it has been shown that levetiracetam does not influence synaptic current or calcium oscillations on acute exposure at 100 μM [8], [15], [16], findings consistent with our observations.

289 Brivaracetam also caused little change in calcium oscillations because the target of
290 brivaracetam is the same as levetiracetam [17], [18].
291 Recently, a drug screening method for detecting seizures has been reported using features
292 extracted from electrical activities of neuronal networks determined by a multi-electrode
293 array (MEA) [19], [20]. To analyze MoAs of compounds, we propose an experimental
294 flow that can evaluate hundreds or thousands of compounds, to narrow down candidates
295 for detailed analysis using MEA or other assays to evaluate additional features.
296 Our waveform analysis can also be combined with other analyses. For example,
297 simultaneous measurement using MEA can reveal the relationship between calcium
298 dynamics and electrical activity. It can also be combined with indicators of other ions and
299 transmitters to reveal novel aspects of neurophysiology.
300 Furthermore, our method might become a useful tool for evaluating drugs like
301 antidepressants, which modulate neuronal activity, as it has been reported that the pattern
302 of calcium oscillation was modified by addition of MK801, an inhibitor of NMDA
303 receptors [8].
304 In conclusion, the present study showed changes in the number and shape of calcium
305 oscillations, representing characteristics of various AEDs. In our method, cultured
306 neurons can be replaced by neurons from model mice or iPS cell-derived neurons to
307 reproduce pathologies. The measurement and analysis methods we describe here will be
308 useful for characterizing and predicting MoAs of novel and existing CNS drugs, including
309 AEDs.
310
311

312 # Acknowledgments

We deeply appreciate Mr. Yusuke Kakumoto for advising on the statistical analyses, Mr. Hiroki Fukuta, Dr. Takahito Inoue, Dr. Tetsutaro Sumiyoshi and Dr. Yosuke Nao for preparing primary cells dissociated from neonatal rats.

[1] K. Fujimori *et al.*, "Modeling sporadic ALS in iPSC-derived motor neurons identifies a potential therapeutic agent," *Nat. Med.*, vol. 24, no. 10, pp. 1579–1589, 2018, doi: 10.1038/s41591-018-0140-5.

[2] T. Chernov-Rogan *et al.*, "Mechanism-specific assay design facilitates the discovery of Nav1.7-selective inhibitors," *Proc. Natl. Acad. Sci. U. S. A.*, vol. 115, no. 4, pp. E792–E801, 2018, doi: 10.1073/pnas.1713701115.

[3] E. Hegstad, I. A. Langmoen, and J. J. Hablitz, "Zinc and glycine do not modify low-magnesium-induced epileptiform activity in," *Epilepsy Res.*, vol. 3, pp. 174–177, 1989.

[4] D. Smetters, A. Majewska, and R. Yuste, "Detecting action potentials in neuronal populations with calcium imaging," *Methods A Companion to Methods Enzymol.*, vol. 18, no. 2, pp. 215–221, 1999, doi: 10.1006/meth.1999.0774.

[5] T. Tanaka, H. Saito, and N. Matsuki, "Intracellular calcium oscillation in cultured rat hippocamp al neurons: A model for glutamatergic neurotransmission," *Jpn. J. Pharmacol.*, vol. 70, no. 1, pp. 89–93, 1996, doi: 10.1254/jjp.70.89.

[6] H. P. C. Robinson, M. Kawahara, Y. Jimbo, K. Torimitsu, Y. Kuroda, and A. Kawana, "Periodic synchronized bursting and intracellular calcium transients elicited by low magnesium in cultured cortical neurons," *J. Neurophysiol.*, vol. 70, no. 4, pp. 1606–1616, 1993, doi: 10.1152/jn.1993.70.4.1606.

337 [7] M. Shen, T. M. Piser, V. S. Seybold, and S. A. Thayer, "Cannabinoid receptor
338 agonists inhibit glutamatergic synaptic transmission in rat hippocampal cultures,"
339 *J. Neurosci.*, vol. 16, no. 14, pp. 4322–4334, 1996, doi: 10.1523/jneurosci.16-14-
340 04322.1996.
341 [8] N. Pacico and A. M. Le Meur, "New in vitro phenotypic assay for epilepsy:
342 Fluorescent measurement of synchronized neuronal calcium oscillations," *PLoS*
343 *One*, vol. 9, no. 1, 2014, doi: 10.1371/journal.pone.0084755.
344 [9] K. Hemstapat, M. T. Smith, and G. R. Monteith, "Measurement of intracellular
345 Ca2+ in cultured rat embryonic hippocampal neurons using a fluorescence
346 microplate reader: Potential application to biomolecular screening," *J.*
347 *Pharmacol. Toxicol. Methods*, vol. 49, no. 2, pp. 81–87, 2004, doi:
348 10.1016/j.vascn.2003.10.002.
349 [10] X. S. Wang and E. I. Gruenstein, "Mechanism of synchronized Ca2+ oscillations
350 in cortical neurons," *Brain Res.*, vol. 767, no. 2, pp. 239–249, 1997, doi:
351 10.1016/S0006-8993(97)00585-4.
352 [11] G. R. Richards, A. D. Jack, A. Platts, and P. B. Simpson, "Measurement and
353 Analysis of Calcium Signaling in Heterogeneous Cell Cultures," *Methods*
354 *Enzymol.*, vol. 414, no. 06, pp. 335–347, 2006, doi: 10.1016/S0076-
355 6879(06)14019-7.
356 [12] A. Reimers, J. A. Berg, M. L. Burns, E. Brodtkorb, S. I. Johannessen, and C. J.
357 Landmark, "Reference ranges for antiepileptic drugs revisited: A practical
358 approach to establish national guidelines," *Drug Des. Devel. Ther.*, vol. 12, pp.
359 271–280, 2018, doi: 10.2147/DDDT.S154388.
360 [13] S. Yoshida, M. Okada, G. Zhu, and S. Kaneko, "Carbamazepine prevents

breakdown of neurotransmitter release induced by hyperactivation of ryanodine receptor," *Neuropharmacology*, vol. 52, no. 7, pp. 1538–1546, 2007, doi: 10.1016/j.neuropharm.2007.02.009.

[14] P. Granger *et al.*, "Modulation of the γ-aminobutyric acid type A receptor by the antiepileptic drugs carbamazepine and phenytoin," *Mol. Pharmacol.*, vol. 47, no. 6, pp. 1189–1196, 1995.

[15] A. Gorji *et al.*, "Effect of levetiracetam on epileptiform discharges in human neocortical slices," *Epilepsia*, vol. 43, no. 12, pp. 1480–1487, 2002, doi: 10.1046/j.1528-1157.2002.23702.x.

[16] X. F. Yang, A. Weisenfeld, and S. M. Rothman, "Prolonged exposure to levetiracetam reveals a presynaptic effect on neurotransmission," *Epilepsia*, vol. 48, no. 10, pp. 1861–1869, 2007, doi: 10.1111/j.1528-1167.2006.01132.x.

[17] A. Matagne, D. Margineanu, B. Kenda, P. Michel, and H. Klitgaard, "Anti-convulsive and anti-epileptic properties of brivaracetam (ucb 34714), a high-affinity ligand for the synaptic vesicle protein , SV2A," no. December 2007, pp. 1662–1671, 2008, doi: 10.1038/bjp.2008.198.

[18] B. A. Lynch *et al.*, "The synaptic vesicle is the protein SV2A is the binding site for the antiepileptic drug levetiracetam," *Proc. Natl. Acad. Sci. U. S. A.*, vol. 101, no. 26, pp. 9861–9866, 2004, doi: 10.1073/pnas.0308208101.

[19] A. M. Tukker, F. M. J. Wijnolts, A. de Groot, and R. H. S. Westerink, "Applicability of hipsc-derived neuronal cocultures and rodent primary cortical cultures for in vitro seizure liability assessment," *Toxicol. Sci.*, vol. 178, no. 1, pp. 71–87, 2020, doi: 10.1093/toxsci/kfaa136.

[20] A. Odawara, N. Matsuda, Y. Ishibashi, R. Yokoi, and I. Suzuki, "Toxicological

385 evaluation of convulsant and anticonvulsant drugs in human induced pluripotent
386 stem cell-derived cortical neuronal networks using an MEA system," *Sci. Rep.*,
387 vol. 8, no. 1, pp. 1–11, 2018, doi: 10.1038/s41598-018-28835-7.
388

A

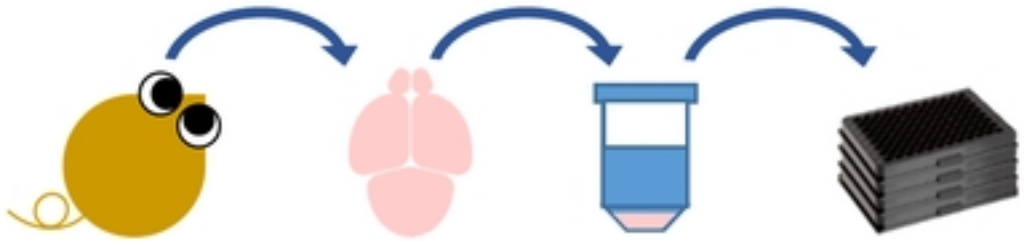

Culture for 14 days

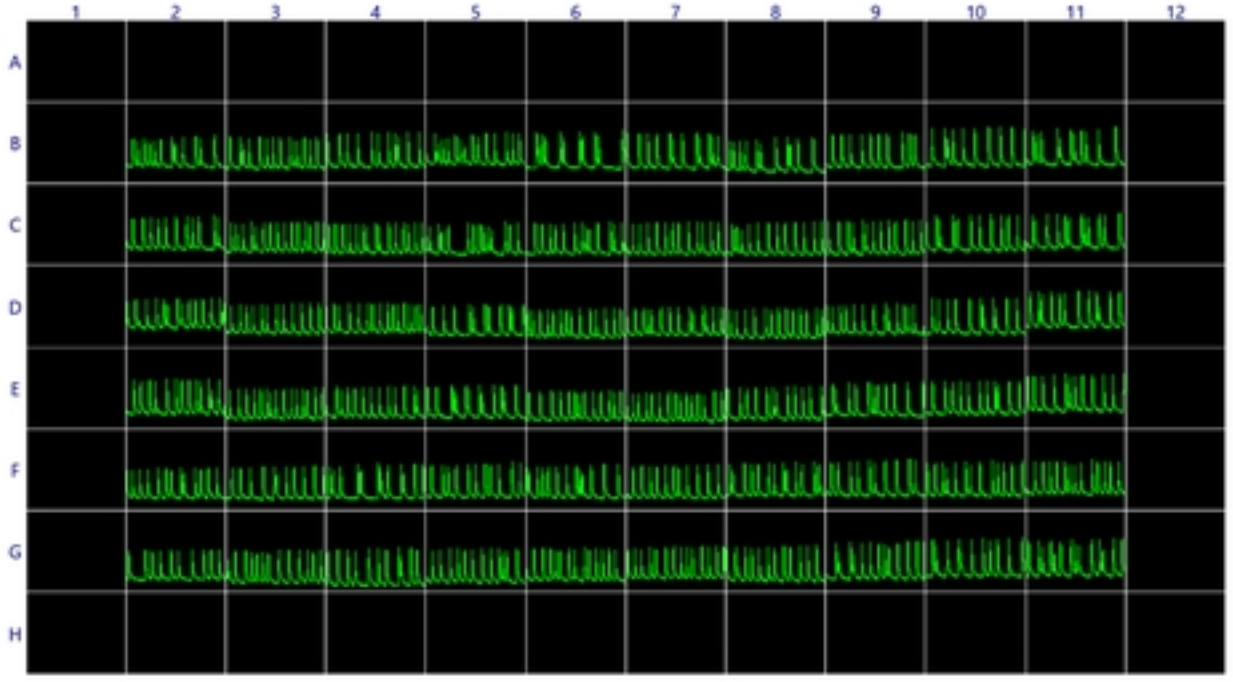

B

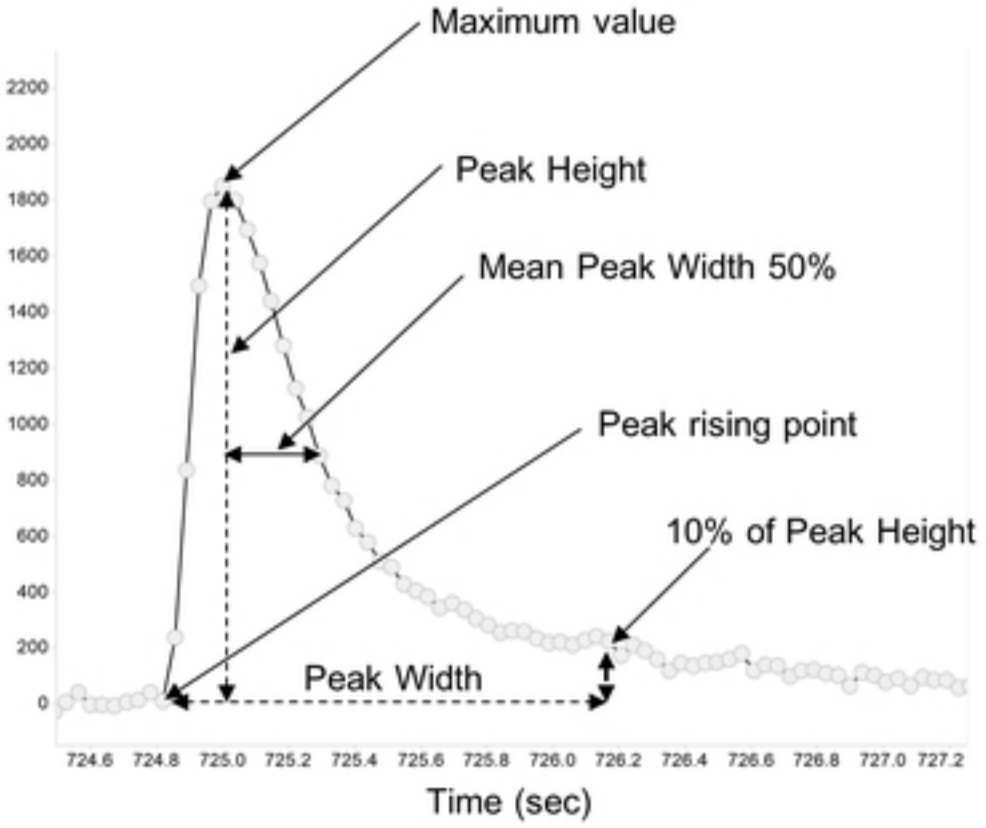

C

Features
Mean Peak Height
CV (coefficient of variation) of Peak Height
Mean Peak Height / Peak Width
Mean Peak Width 50%
AUC
Peak Number

Figure1

A

Compound	Main mechanism
Levetiracetam	SV2A modulator
Brivaracetam	SV2A modulator
Perampanel	AMPA receptor antagonist
Diazepam	$GABA_A$ receptor agonist
Clonazepam	$GABA_A$ receptor agonist
Carbamazepine	Voltage-gated sodium channel inhibitor
Lamotrigine	Voltage-gated sodium channel inhibitor
Lacosamide	Voltage-gated sodium channel inhibitor

B

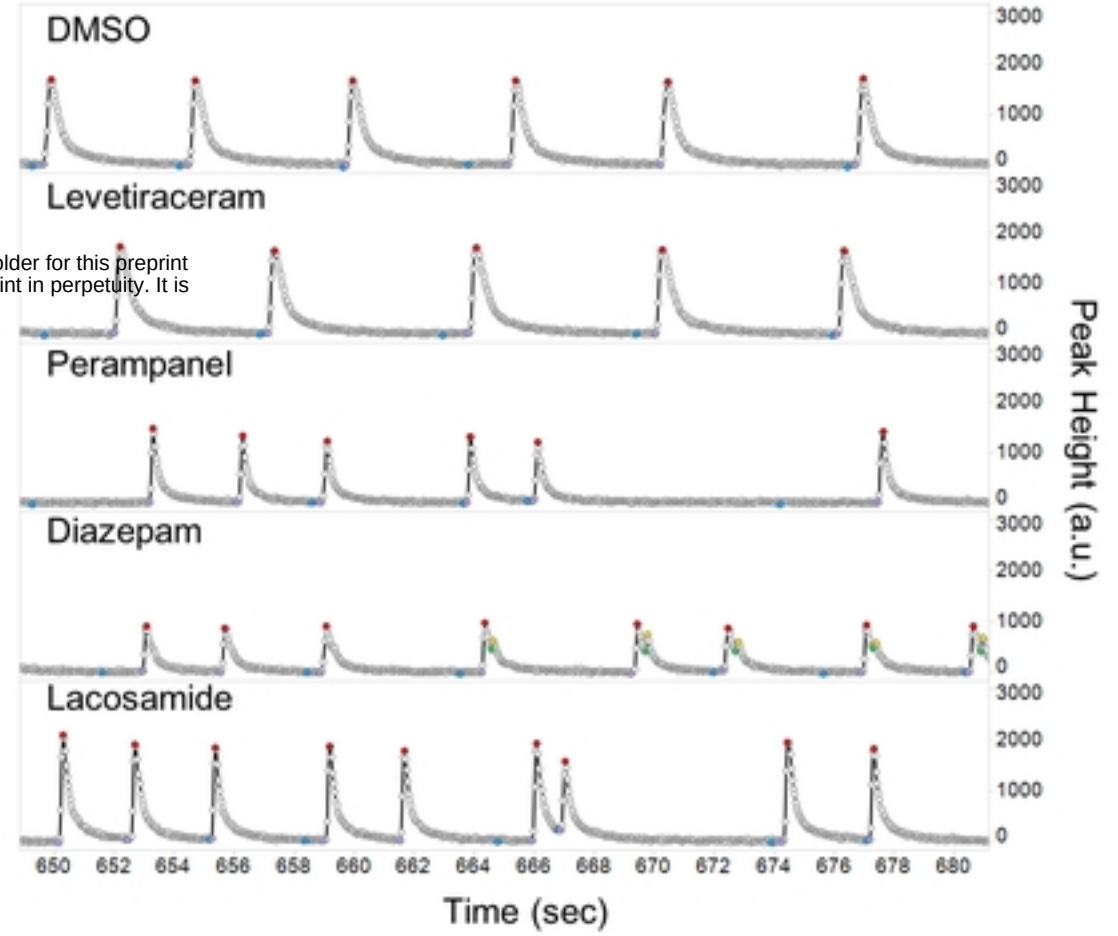

C

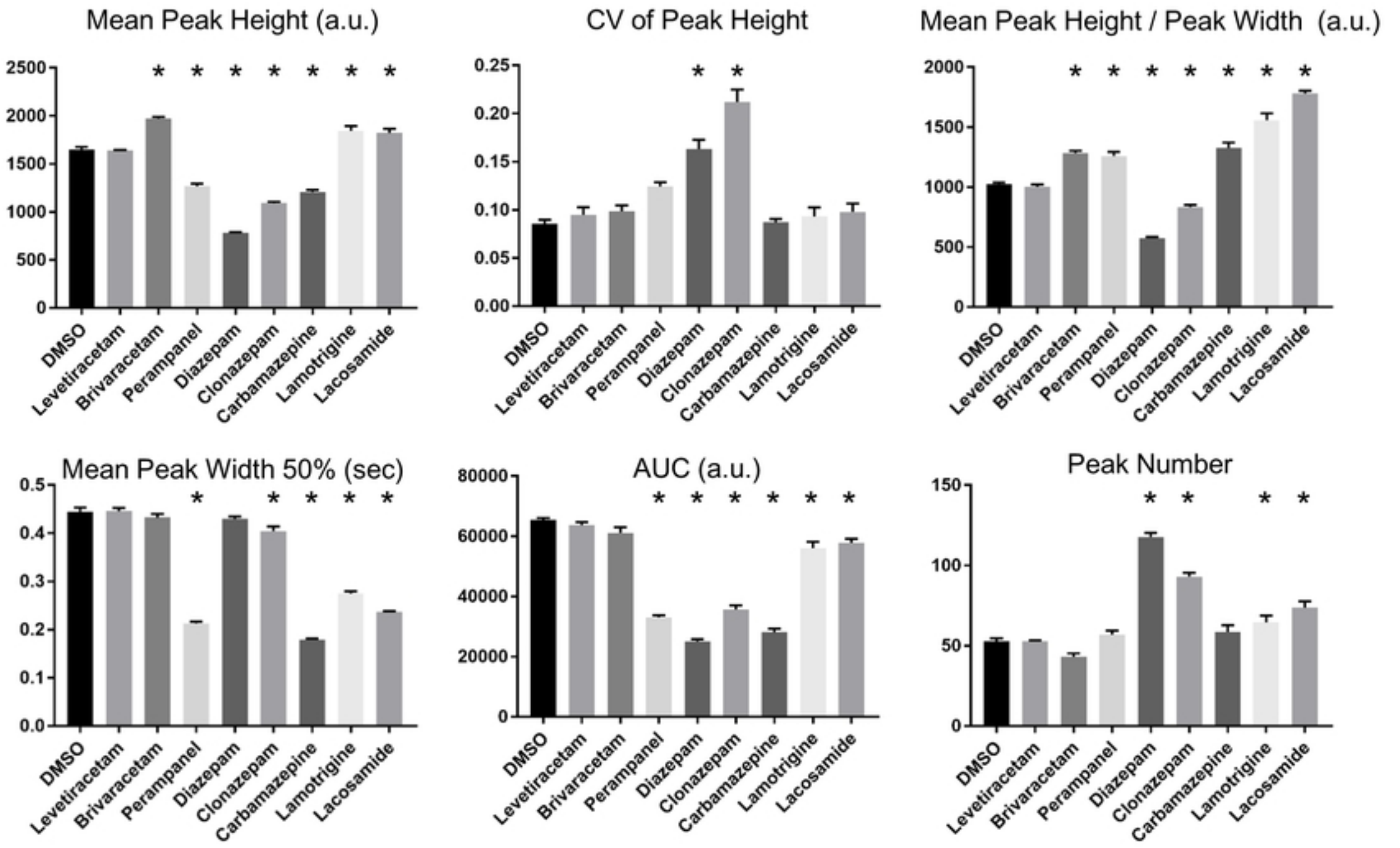

Figure2

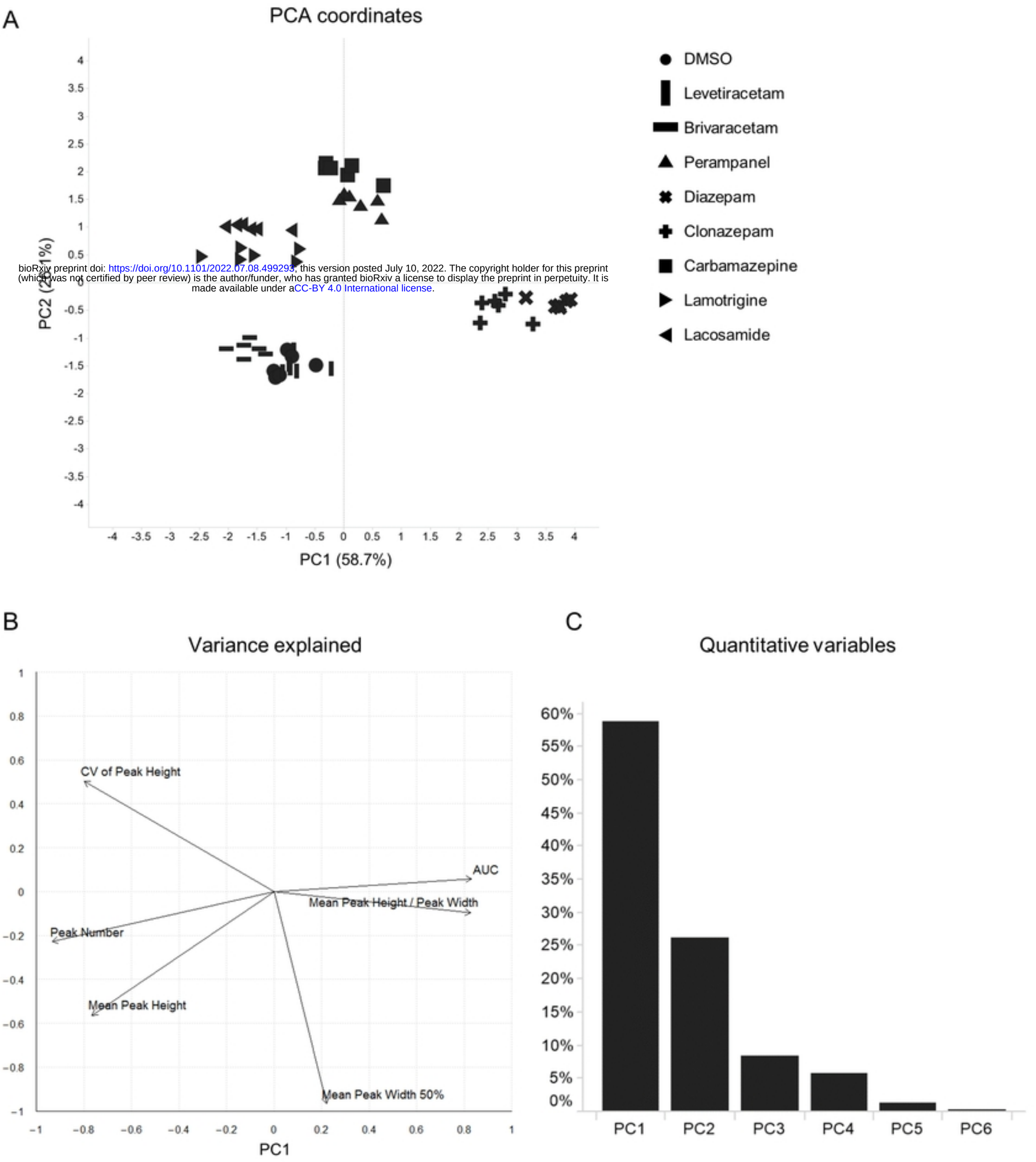

Figure3

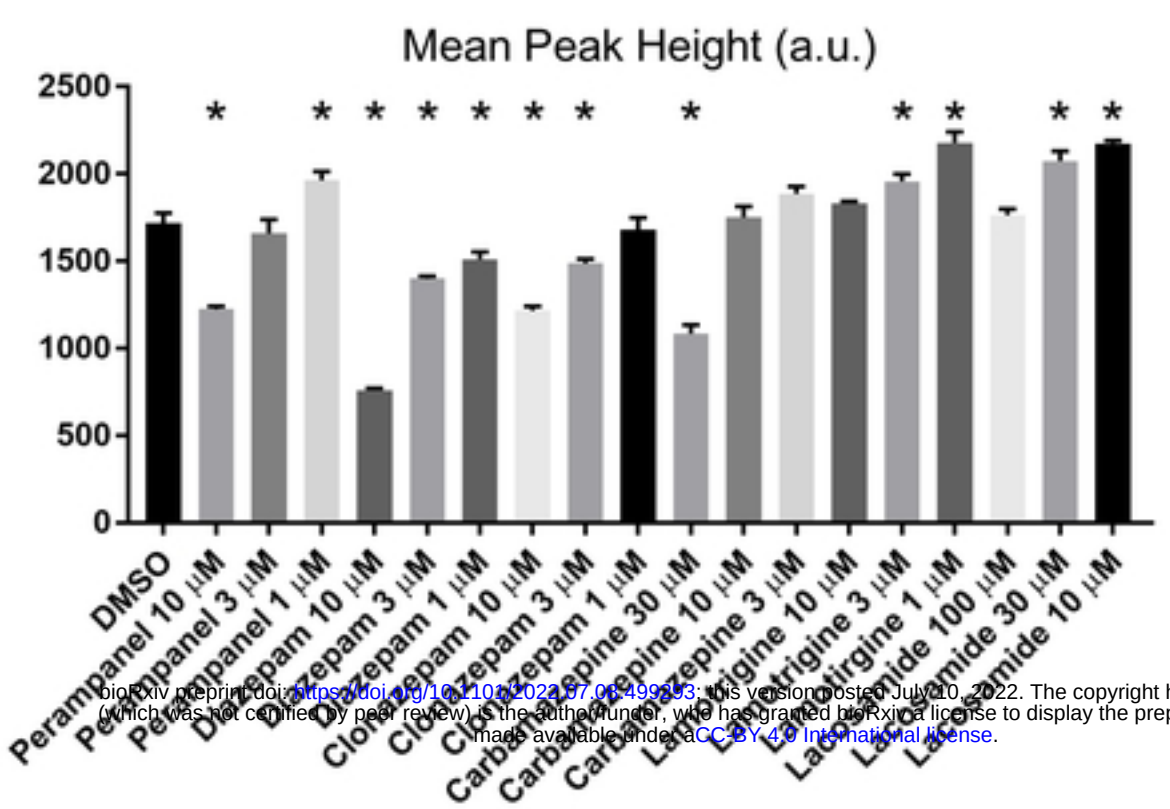

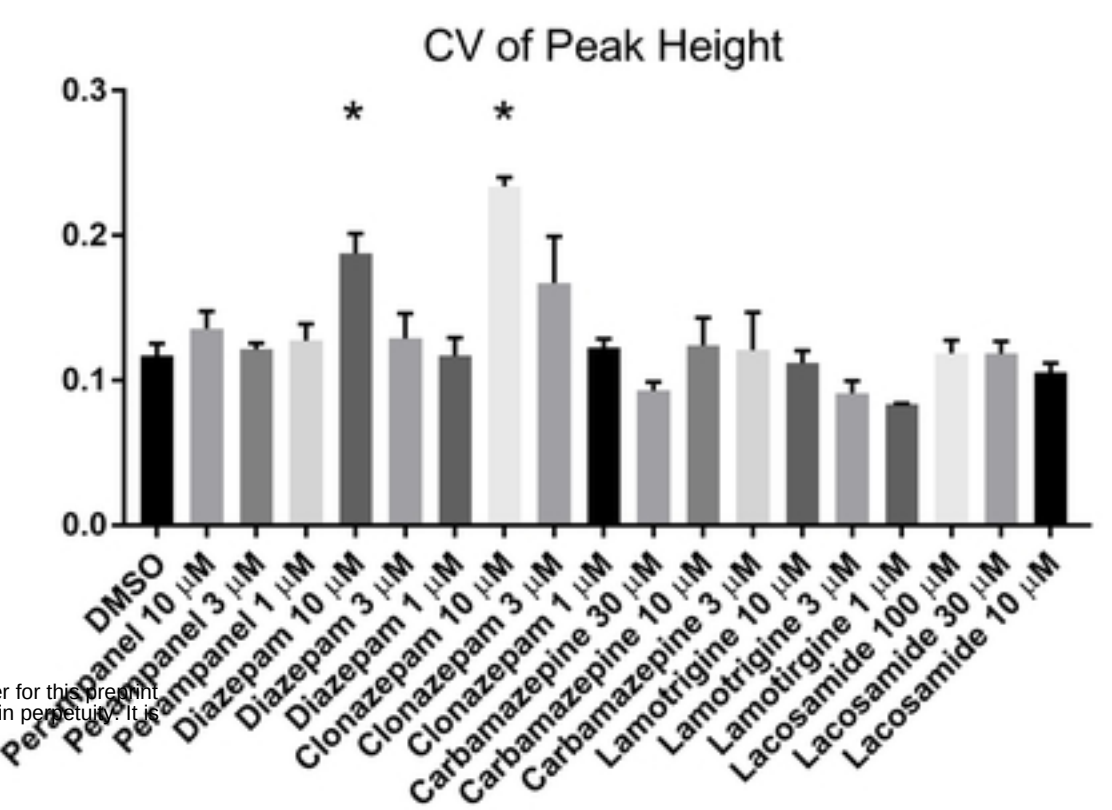

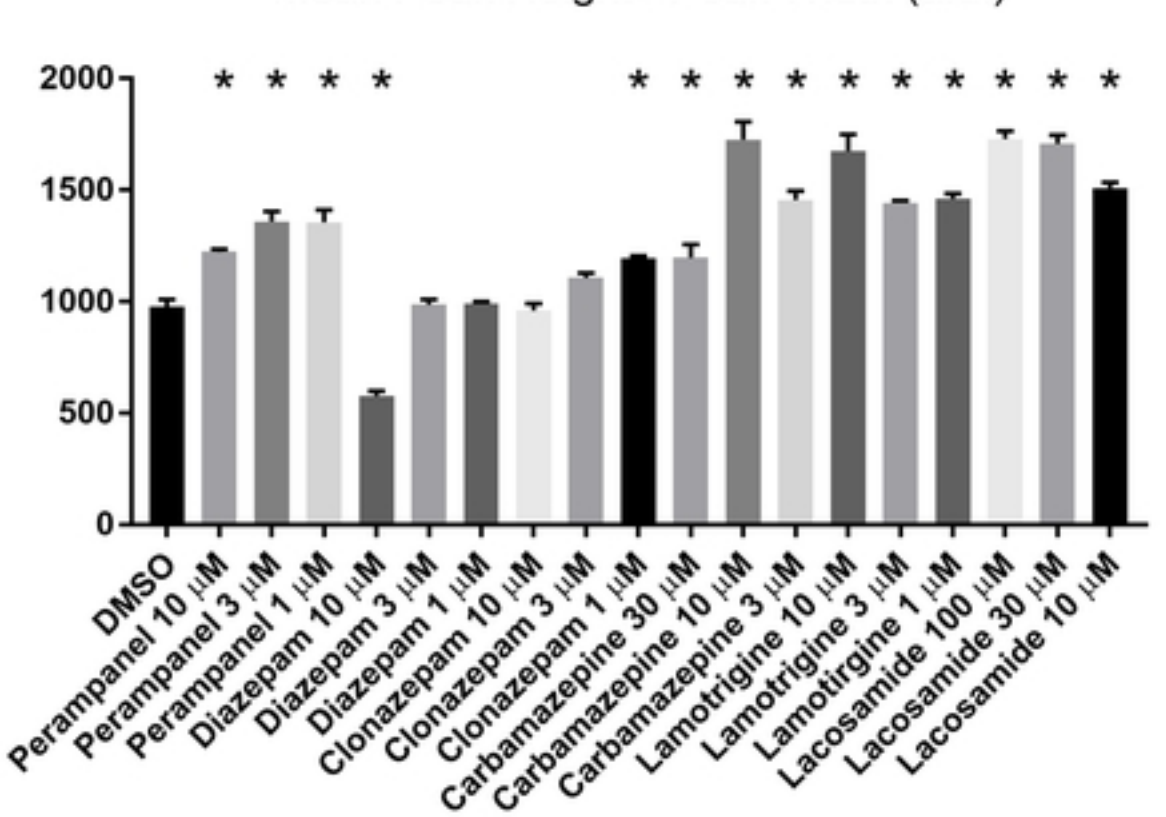

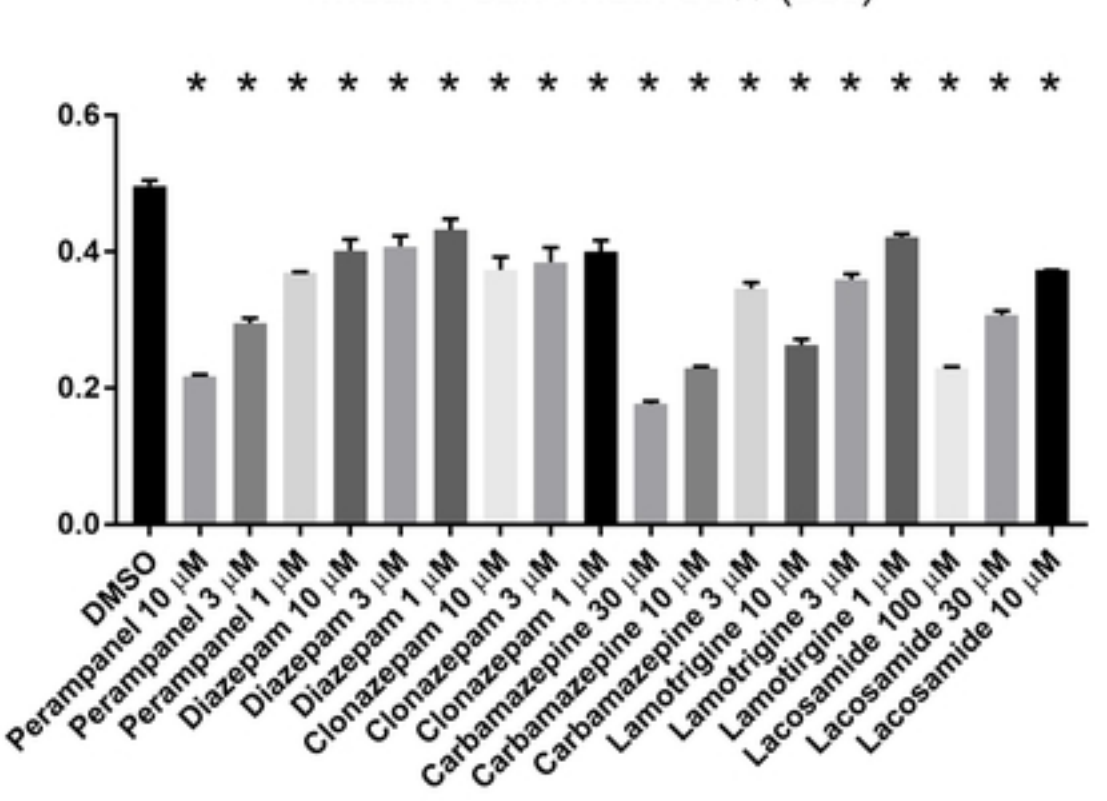

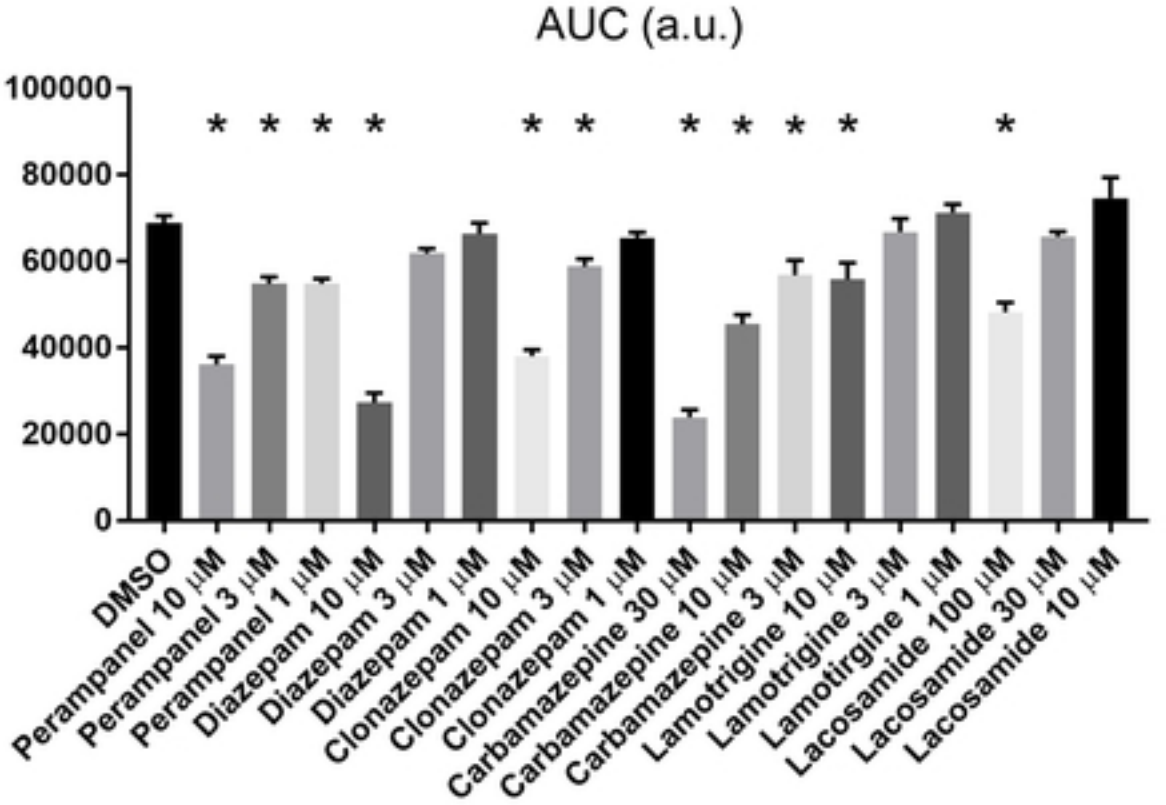

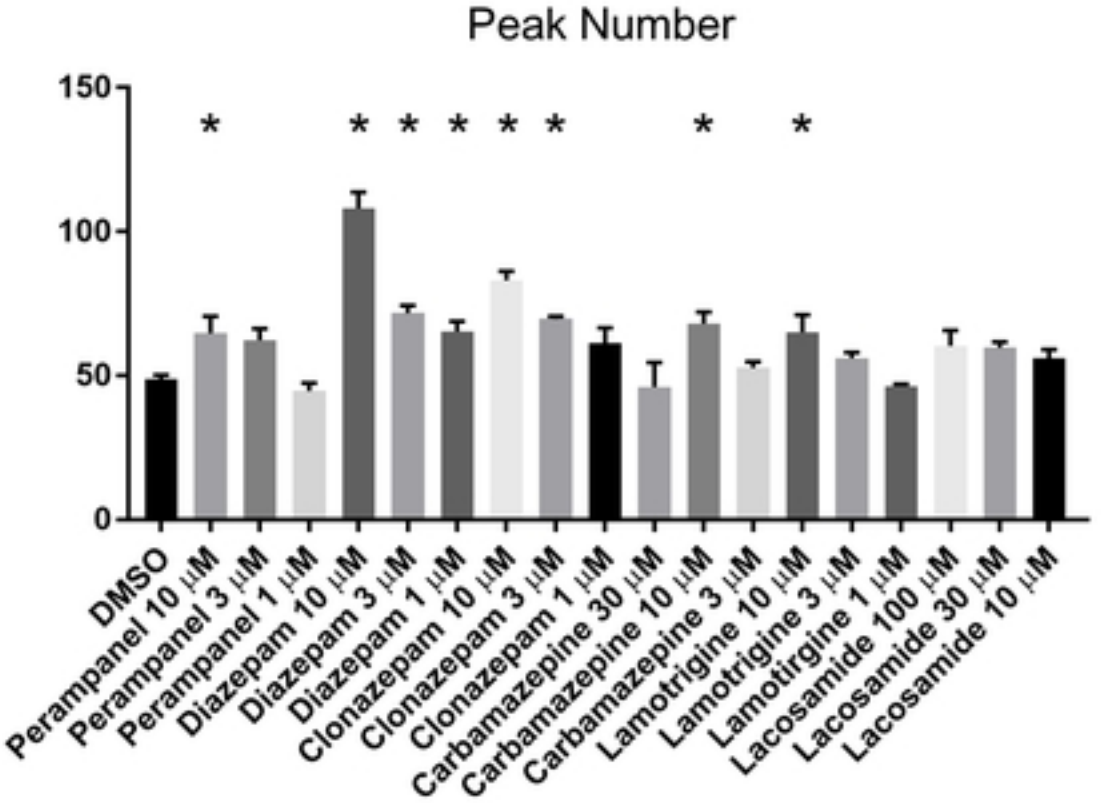

Figure4

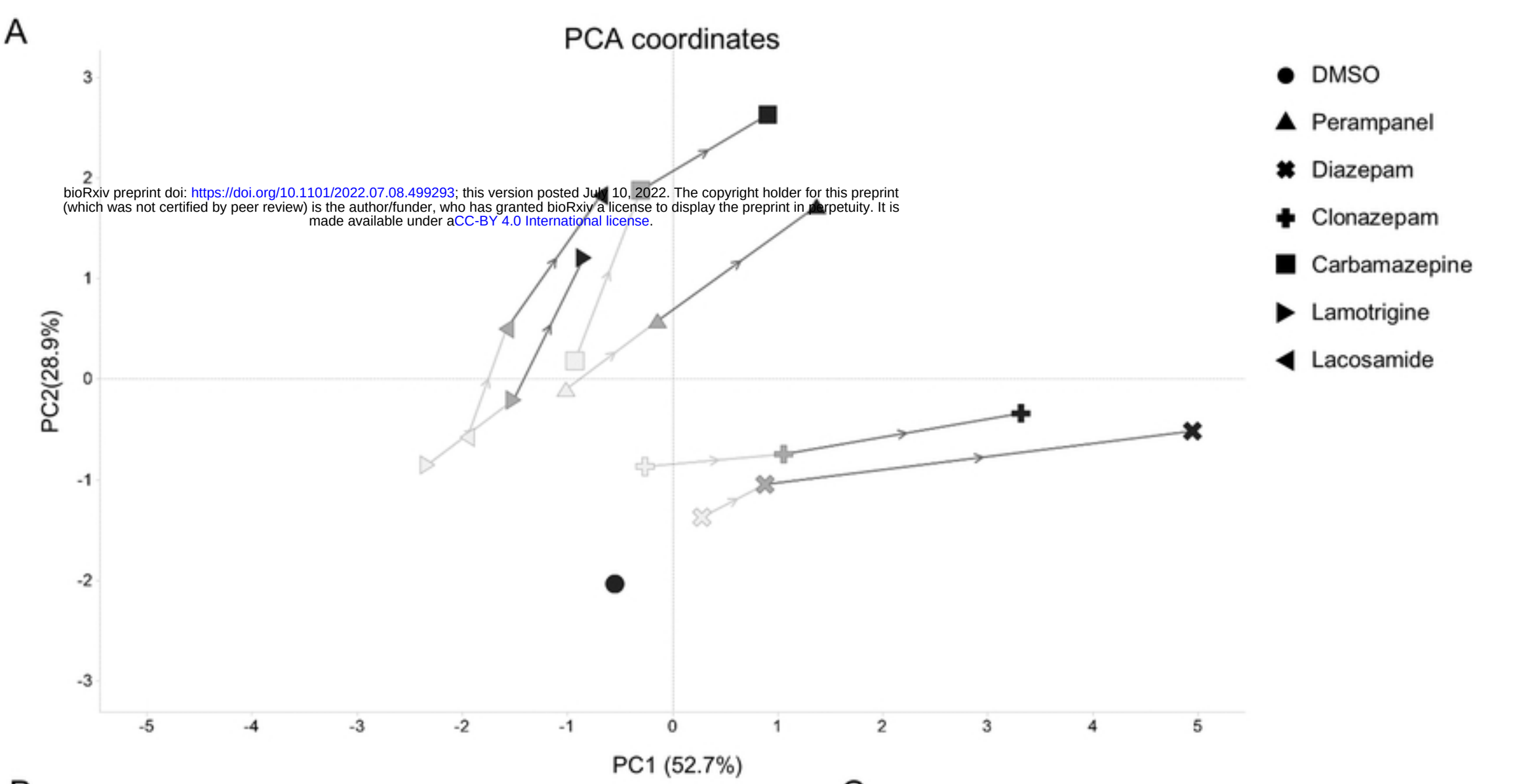

Figure5